TNF counterbalances the emergence of M2 tumor macrophages

Franz Kratochvill et al.

Supplemental Material

Index

Antibodies (related to Methods)

For flow cytometry the following antibodies were used: Anti-mouse MHC II (I-A/I-E; clone M5/114.15.2; eBioscience), anti-mouse/human CD11b (clone M1/70, BioLegend), anti-mouse Ly6C (clone HK1.4, BioLegend), anti-mouse Ly6G (clone 1A8 BioLegend), anti-mouse IL-13Rα (clone 10MOKA, eBioscience), anti-mouse IL-4Rα (CD124; BD Bioscience), anti-mouse F4/80 (Clone BM8; BioLegend), rat anti-mouse SiglecF (clone E50-2440; BD Biosciences), anti-mouse CD8a (Clone 53-6.7; BioLegend), anti-mouse CD3 (Clone 17A2; BioLegend), anti-mouse CD4 (Clone IM7; BioLegend), anti-mouse PD-L2 (CD273; clone TY25; BioLegend). For immunoblotting the following antibodies were used: Myd88 (D80F5, Cell Signaling) and chicken anti-ARG1 (gift from Sid Morris, University of Pittsburgh). Equal loading was controlled by using anti mouse GRB2 antibody (cat. no. 610112, BD Bioscience).

Tumor sphere model – in vitro (related to Methods)

The TT9423 neuroblastoma cell line (gift from J. Lahti) was grown as a monolayer in vitro in complete RPMI (Corning) containing 10% fetal bovine serum (Thermo Scientific), 1% penicillin/streptomycin (Invitrogen), and 0.1% gentamycin (Invitrogen). TT9423 cells were collected from the tissue culture plate using trypsin-EDTA (Invitrogen), and $1x10^5$ cells were transferred to tissue culture plates coated with 0.5% agar noble in RPMI for overnight sphere development. Subsequent to sphere formation, bone marrow-derived macrophages (BMDMs) were added to the same cell number as TT9423 cells originating the sphere cultures. Sphere and BMDMs (ivTAMs) were co-cultured for 24 to 72 hours and then further analyzed.

Microarray and computational analysis(related to Methods)

RNA was prepared using TRIZOL from sorted or unsorted TAMs. RNA processing steps of target labeling and hybridization to HT_MG430_PM or Mouse Gene 2.0 ST arrays (both Affymetrix). RNA quality was confirmed by analysis on the Agilent 2100 Bioanalyzer. For samples analyzed on HT_MG430_PM arrays, biotin-labeled targets were generated from 100 ng total mouse RNA using the Affymetrix 3'IVT Express assay (P/N 901225). For samples analyzed on Mouse Gene 2.0 ST arrays, biotin labeled targets were generated from 100 ng total

mouse RNA using the Ambion® WT Expression Kit (Life Technologies P/N 4411973) and the Affymetrix® GeneChip® WT Terminal Labeling Kit (Affymetrix P/N 900671). 5 µg of labeled targets were hybridized overnight to Affymetrix arrays then processed using the Affymetrix GeneTitan system (HT_MG430_PM arrays) or using automated GeneChip 450 fluidics modules and 7000G scanner (Mouse Gene 2.0 ST arrays). Signals from scanned arrays were summarized to transcript (probe set) measures using the RMA algorithm (Affymetrix Expression Console v1.1) and then converted to linear signals by exponentiation (base 2). Probe set annotations were obtained from the Affymetrix NetAffx website. Gene expression values were calculated as the maximum signal across redundant probe sets and are reported as the mean signal +/- SEM. In some cases, array data were manually annotated following ranking based on expression level, or annotated based on Gene Ontology terms.

qRT-PCR primers (related to Methods)

IL-6	Primer 1: GGGAAATCGTGGAAATGAGA
	Primer 2: CCAGTTTGGTAGCATCCATCA
IL12p40	Primer 1: CCAGTTTGGTAGCATCCATCA
	Primer 2: AACTTGAGGGAGAAGTAGGAATGG
IL-23p19	Primer 1: CAAGGACAACAGCCAGTTC
	Primer 2: CCATGGGGCTATCAGGGAGTA
G-CSF	Primer 1: CAACTTTGCCACCACCATCT
	Primer 2: GCTGGAAGGCAGAAGTGAAG
Ccl24	QuantiTect Primer Assay QT00126021 (Qiagen)
Ccl17	QuantiTect Primer Assay QT00131572 (Qiagen)
Mgl2	QuantiTect Primer Assay QT00143640 (Qiagen)
Mrc1	QuantiTect Primer Assay QT00103012 (Qiagen)
IL-13	QuantiTect Primer Assay QT00099554 (Qiagen)
Ccl22	QuantiTect Primer Assay QT00108031 (Qiagen)
Arg1	Primer 1: ACAGTCTGGCAGTTGGAAGCATC
	Primer 2: GGGAGTCCCCAGGAGAATCCT
	Probe: CTGGCCACGCCAGGGTCCAC
Nos2	Primer 1: TGCCCCTTCAATGGTTGGTA

	Primer 2: ACTGGAGGGACCAGCCAAAT
	Probe: CGCTACAACATCCTGGAGGAAGTGG
IL-27	Primer 1: GGCCATGAGGCTGGATCTC
	Primer 2: AACATTTGAATCCTGCAGCCA
Retnla	Primer 1: TCGTGGAGAATAAGGTCAAGG
	Primer 2: GGAGGCCCATCTGTTCATAG
TNF	Primer 1: AAAATTCGAGTGACAAGCCTGTAGC
	Primer 2: GTGGGTGAGGAGCACGTAG
IL-1α	Primer 1: TCTGAAGAAGAGACGGCTGA
	Primer 2: CTGATCTGGGTTGGATGGTC
IL-1β	Primer 1: ACGGACCCCAAAAGATGAAG
	Primer 2: TACTGCCTGCCTGAAGCTCT
IL-10	Primer 1: CCCAAGTAACCCTTAAAGTCCTGC
	Primer 2: ATGCTGCCTGCTCTTACTGACTG
KC	Primer 1: ACTCAAGAATGGTCGCGAGG
	Primer 2: GCA GTC TGT CTT CTT TCT CCG
Gapdh	Primer/probe mix from Applied Biosystems

Supplemental Figure legends

Supplementary Figure 1. Rapid and efficient TAM isolation from different mouse tumor models (related to Figure 1)

(A) Schematic of enrichment of TAMs from tumors by digestion, percoll gradient separation and $CD11b^+$ magnetic cell sorting (MACS). $CD11b^+$ cells following magnetic sorting from 4 different tumor models (G: glioma; T: Thymoma; N: Neuroblastoma; R: Retinoblastoma) were analyzed by cytospin. (B) qRT-PCR analysis of $CD11b^+$ TAMs after isolation (-; $n \geq 8$) or rested on tissue culture (TC; $n = 8$) dishes for 24 h after isolation. Data represent TAMs from individual mice from 2 experiments. Mean expression is shown with error bars +/- SEM. (C) Mouse NB-spheres cultured with BMDMs analyzed by immunohistochemistry. (D) ivTAMs and bone marrow-derived macrophages (BMDMs) grown on agar coated plates were analyzed by microarray ($n = 3$, GEO accession GSE68817). (E) TNF mRNA expression assessed by qRT-

PCR in resting (i.e. no stimulation by TLR agonists) BMDMs grown on tissue culture dishes (BMDMs), BMDMs cultured on agar (Agar BMDMs) or ivTAMs isolated from the tumor spheres by the same digestion and magnetic bead isolation as used for in vivo TAMs, and immediately lysed for RNA. Data are the mean expression values from individual mice (n = 2) representing 1 out of 3 experiments. Error bars, SEM. Statistical significance is indicated by *p< 0.05, **p< 0.01 and ***p< 0.001.

Supplementary Figure 2. CD11b^{+} TAMs have an MyD88-independent inflammatory expression profile (related to Figure 1)

(A) TLR and IL1R expression in CD11b^{+} TAMs derived from microarray data where the highest mean probe set expression was plotted (n = 3 per tumor TAM type). (B) Whole transcriptome analysis of EG7 TAMs derived from *Myd88*$^{-/-}$ and WT littermates (n = 5). Depicted values are heat maps ordered by signal intensities and are representative of 2 independent experiments. (C) Expression of selected targets from microarray data previously shown to be MyD88-dependent in in vitro BMDM culture systems. Numbers within the heat map are log2 values of signal intensity averaged from n = 5 independent values. (D) qRT-PCR analysis of BMDMs resting (black bars) or stimulated with either IL-4 (blue bars) or LPS + IFN-γ (red bars) for 24 h compared to TAMs from 5 solid tumor models (N, neuroblastoma; R, retinoblastoma; O, osteosarcoma; T, thymoma; G, glioma). Data are the mean expression values (n ≥ 3) representative of at least 2 experiments normalized to resting BMDMs. Black lines are the mean of each group. (E) Immunoblot analysis of MyD88 expression in EG7 TAMs isolated from WT (*Myd88*$^{+/+}$, n = 5), *Myd88*$^{fl/fl}$ LysM-Cre (n = 3) and *Myd88*$^{fl/fl}$ Tie2-Cre (n = 2) mice. The blot was reprobed using GRB2 to assure equal loading and represents 1 out of 2 experiments.

Supplementary Figure 3. TNFR1-deficient macrophages support tumor growth (related to Figure 1)

(A and B) Tumor size of EG7 thymomas grown in WT, TNF^{KO}, DKO (A) and WT and Myd88$^{\Delta H}$ (B) mice (WT: n = 15, TNFR^{KO}: n = 14, DKO: n = 12; WT: n = 8, Myd88$^{\Delta H}$: n = 10). Values represent tumors from individual mice from 5 (A) and 2 (B) experiments analyzed 11 and 12 days post injection, respectively. The mean is shown as black bar. Error bars +/- SEM. (C) Schematic representation of the co-transplantation of EG7 tumor cells and WT or TNFR^{KO}

BMDMs at a ratio of 1:1 into $CCR2^{-/-}$ mice for subsequent analysis of tumor growth. (D) Representative Flow Cytometry of EG7 tumors co-transplanted with BMDMs as shown in (C). Data are representative for 3 experiments (n = 3). (E) Tumor growth of EG7 tumors co-injected with BMDMs as shown in (C). The tumor volumes were calculated 5, 8, 11 and 12 days post transplantation using the formula $(width)^2$ x length x 0.52. The data represent the mean volume +/- SEM of 4 experiments (WT BMDMs: n = 21; $TNFR^{KO}$ BMDMs: n = 22). (F) qRT-PCR analysis of EG7 infiltrating monocytes and neutrophils sorted as shown in Figure 2A and B. Values represent data from individual mice (n = 4) from 1 out of 4 experiments. Error bars +/- SEM. Statistical significance was calculated using a two-tailed Student's t test and is indicated by *p< 0.05, **p< 0.01 and ***p< 0.001.

Supplementary Figure 4. Arg1 expression in TAMs is only partially Stat6 dependent (Panel A related to Figure 3; Panels B-F related to Figure 4)

(A) qRT-PCR analysis of $CD11b^+$ EG7 TAMs in WT and $Stat6^{KO}$ mice (n = 6 per genotype). Values of M2 gene expression were normalized to the corresponding WT. Data shown are the mean expression values representative for 1 out of 2 experiments. Error bars +/- SEM. (B - F) Flow Cytometry analysis of lymphocyte populations in EG7 (B) or LLC tumors (C and D) or tumor-draining lymph nodes (E and F) of LLC tumor bearing WT and $TNFR^{KO}$ mice. Data were combined from 2 (LLC) and 3 (EG7) experiments and represent values from n = 8 (WT and $TNFR^{KO}$, LLC), n = 11 (WT, EG7) and n = 12 ($TNFR^{KO}$, EG7) mice. Note that EG7 tumor cells are $CD3^+$ and therefore CD4 and CD8 enumeration was derived from the total CD3 gate. Mean is shown as black line. Error bar, SEM. Statistical significance is indicated by *p< 0.05, **p< 0.01 and ***p< 0.001.

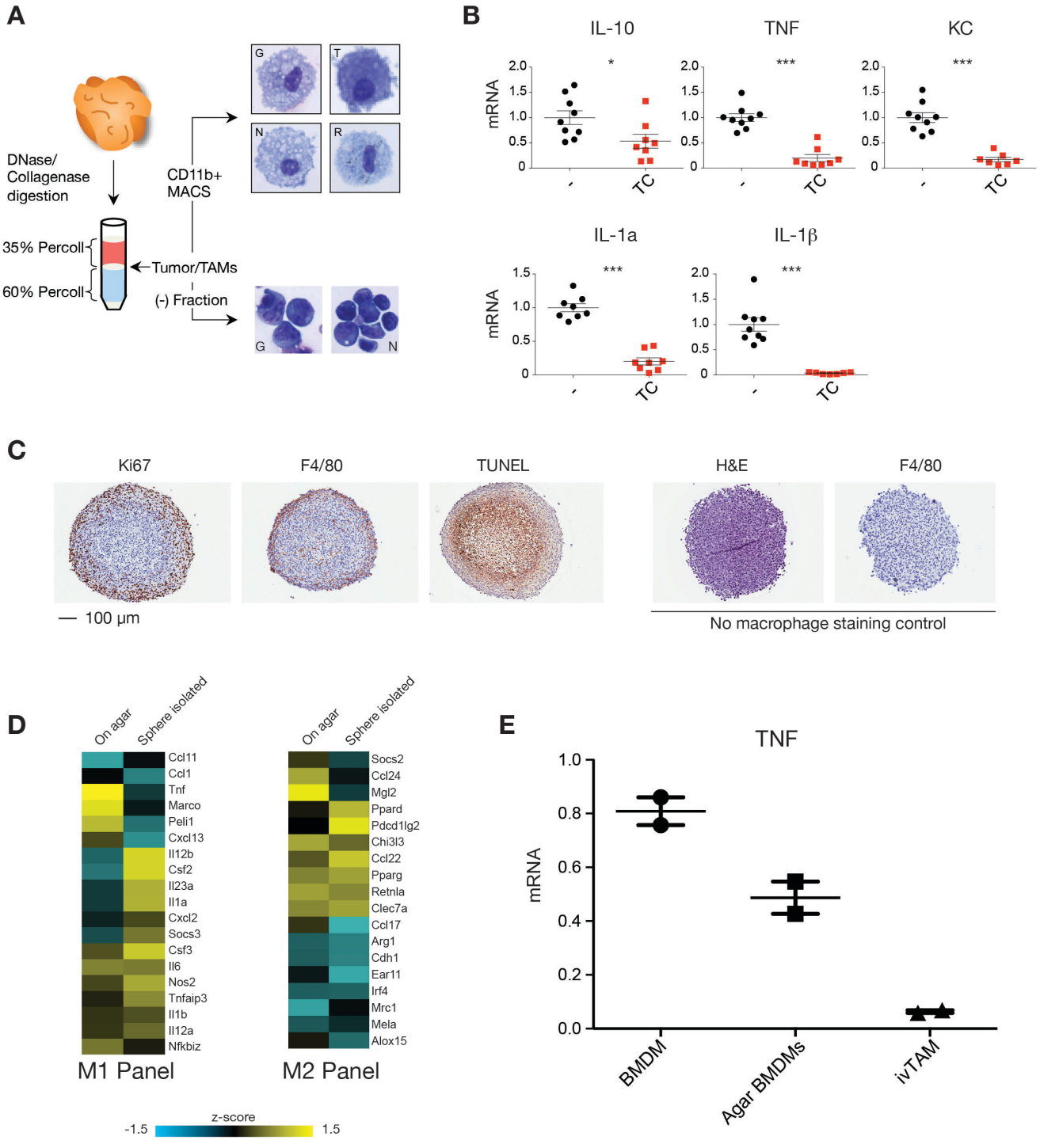

Supplemental Figure 1 (related to Figure 1)

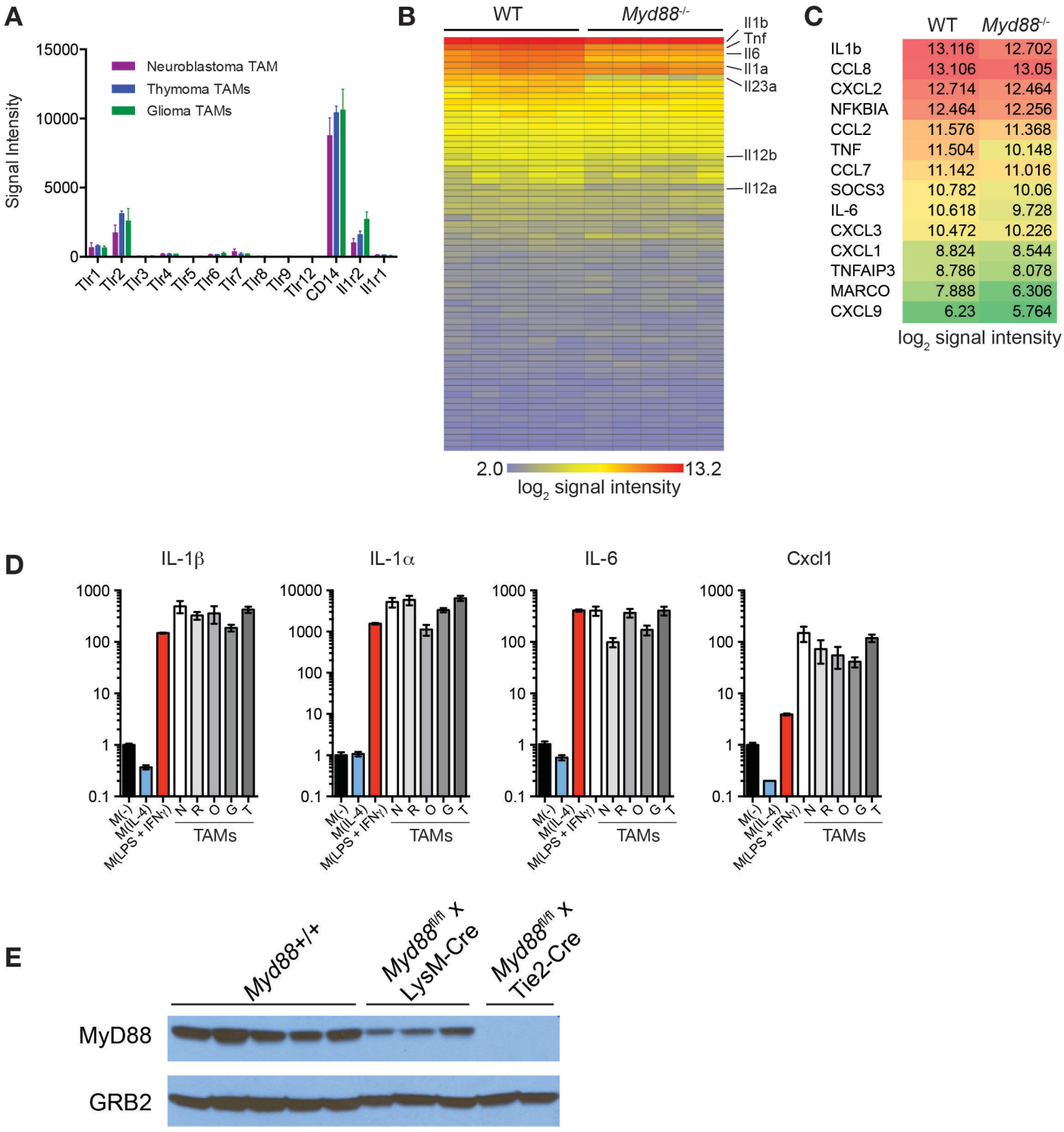

Supplemental Figure 2 (related to Figure 1)

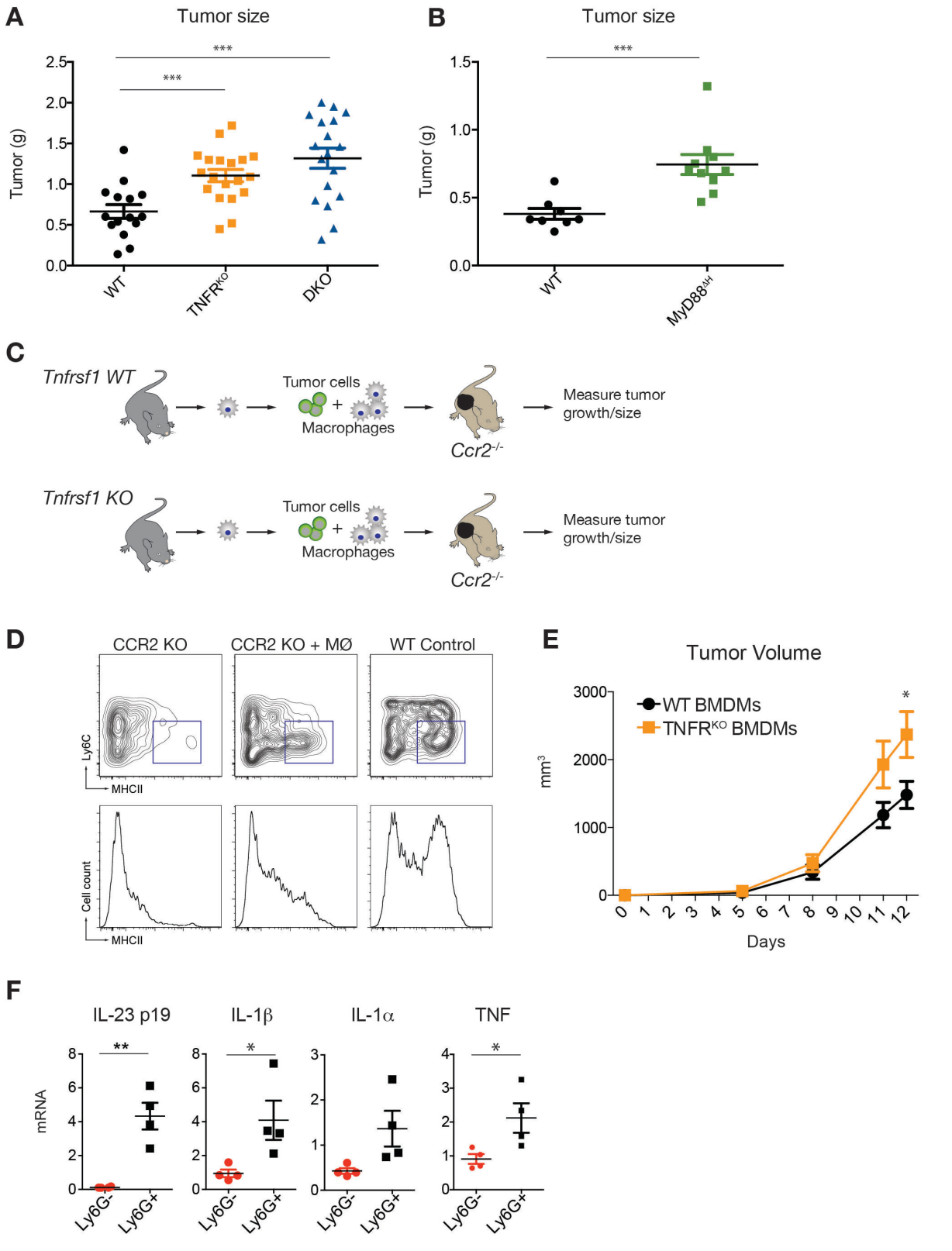

Supplemental Figure 3 (related to Figure 1)

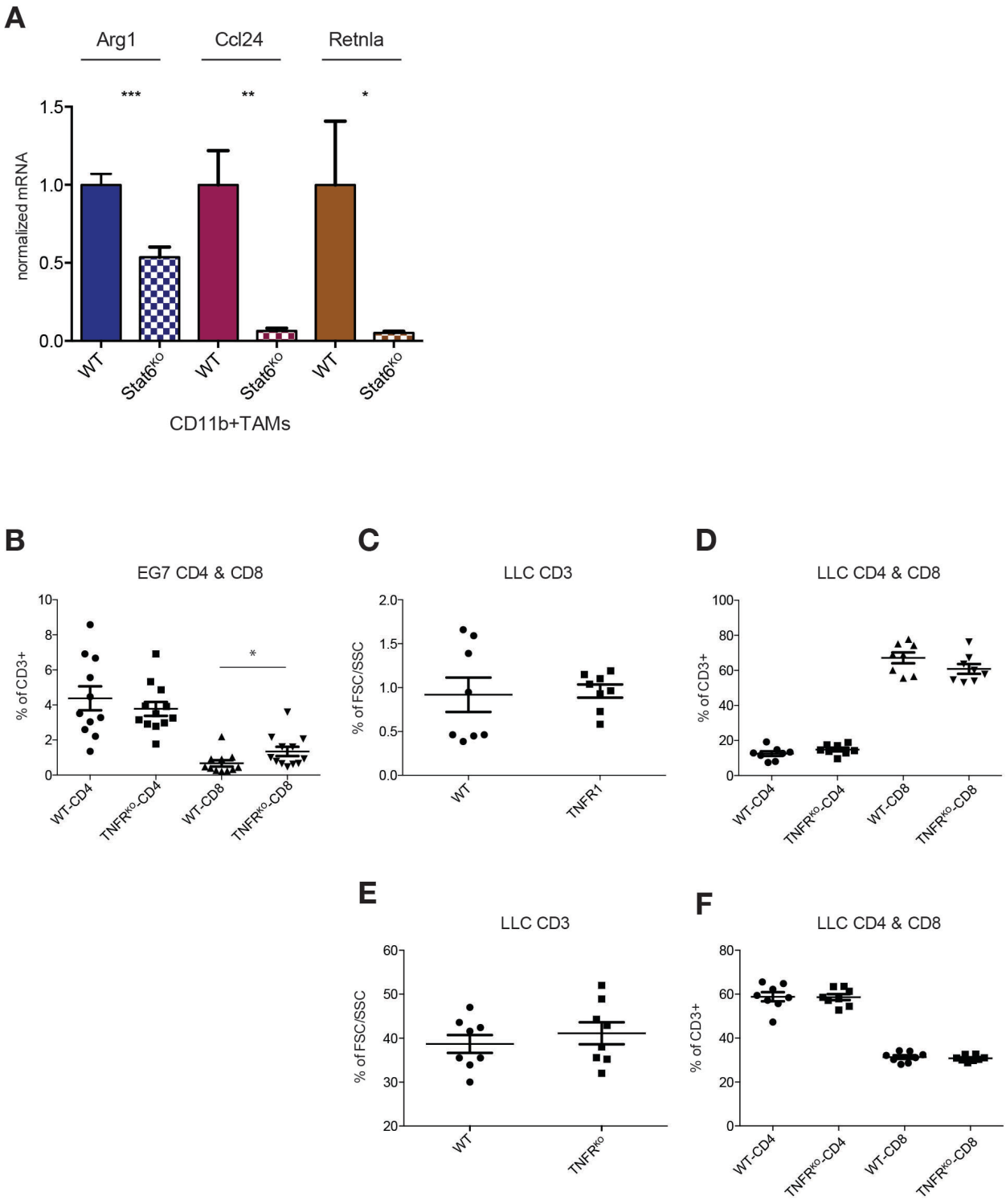

Supplemental Figure 4 (Panel A related to Figure 3; Panels B-F related to Figure 4)